Available online at www.sciencedirect.com
SCIENCE DIRECT
International Journal of Machine Tools & Manufacture 46 (2006) 1079–1086
INTERNATIONAL JOURNAL OF MACHINE TOOLS & MANUFACTURE DESIGN, RESEARCH AND APPLICATION
www.elsevier.com/locate/ijmactool

Reverse engineering of free-form surfaces: A methodology for threshold definition in selective sampling

M. Galetto, E. Vezzetti*

Dipartimento di Sistemi di Produzione Ed Economia dell'Azienda, Politecnico di Torino, Corso Duca degli Abruzzi 24, 10129 Torino, Italy

Received 4 August 2005; accepted 17 August 2005
Available online 23 September 2005

Abstract

Reverse engineering is a technique used during the project phase of a new product, which makes it possible to trace, in terms of mathematical expressions, the geometrical features of a given physical model.

Scientific literature presents many different approaches to reverse engineering. Great part of those are based on the analysis of point clouds acquired through coordinate measuring devices, such as, for example, Coordinate Measuring Machines (CMMs), Optical Scanners or Interferometric Systems.

Referring to this kind of approach, a common problem is to individuate the surface zones, which present sensible variations of curvature. Many algorithms, commonly implemented on commercial software through semi-automatic procedures, are already based on this method. In these cases the local curvature variation of the measured surfaces is analyzed by defining a threshold over which it is necessary to perform a deeper scansion of the surface zones. However, most of the problems are related to the definition of an appropriate value for the threshold level.

In the present paper a methodology for the definition of the threshold value based on the measurement system uncertainty is described. In the current description the method is applied to an elementary algorithm for curvature definition, but it could be extended to any other kind of more complicated approach.

Furthermore, it will be demonstrated that this new methodology is simple to apply and can be easily automated in commercial software for points selective sampling in industrial reverse engineering applications.

In the end a practical example is described in order to give an experimental validation of the method.
© 2005 Elsevier Ltd. All rights reserved.

Keywords: Reverse engineering; Scanning strategy; Geometric morphology

1. Introduction

The development of a new product is an iterative process, which includes: product design, analysis of performance, safety and reliability, product prototyping for experimental evaluation and design modification.

In this process, the first conceptualisation of the new product shape is often obtained with the help of a physical model, which is successively coded in a mathematical expression, in order to give a handier support for the successive development phases. Reverse engineering is one of the most frequent solutions for this kind of conversion.

Starting from a physical model of the new product, using an acquisition device for surface point localisation, reverse engineering is able to digitise the geometric characteristics of the object in the space and then to create a complete mathematical model (in terms of analytical surfaces or solid elements) [1].

It must be said that, even if reverse engineering has a great valence in the project phase and gives a significant help to the lead-time reduction of the entire product development, its use is constrained by the first feasibility study and by the choice of an efficient working space.

In order to better understand the most critical aspects connected to the reverse engineering application, it is opportune to split the entire methodology in three main steps: point digitisation, segmentation and surface

* Corresponding author. Tel.: +39 011 5647294; fax: +39 011 5647299.
E-mail address: enrico.vezzetti@polito.its (E. Vezzetti).

0890-6955/$ - see front matter © 2005 Elsevier Ltd. All rights reserved.
doi:10.1016/j.ijmachtools.2005.08.007

modelling. Focusing the attention on 'point digitisation' and 'surface modelling', some relevant problems associated to the sampling strategy must be highlighted [2].

The surface point digitisation usually starts with a manual digitisation process that is often time consuming and tedious, specially working with complex free-forms. Some commercial systems automate the process by scanning the surface across a rectangular patch with a fixed scanning pitch. However, this method tends to pick up redundant points on relatively flat surfaces or in regions with constant curvature. While at first, working with contact systems, this was a great problem because it asked a long acquisition time, the technological evolution of the acquisition devices has driven to the chance to employ fast non-contact digitisers, such as laser range finders, stereo image detectors, moiré interferometers and structured lighting devices, that can scan dense measurement data in a relatively short time. Even if this could be considered an attractive solution for the problem of scanning strategy choice, the obtained results are not guaranteed in term of measurements accuracy. In fact, if the surface is complex and a very accurate model is required, the use of non-contact acquisition device does not represent the optimal solution. This is due to the strong metrological constraints related to non-contact systems acquisition technology [3].

In addition, the presence of very crowd points clouds, generated from the non-contact devices, obliges to perform a strong data manipulation and filtering in order to lighten the successive elaboration by conventional CAD systems.

Regarding the accuracy of the surface modelling, the minimisation of digitised errors is important in the reconstruction of accurate mathematical surfaces from original physical models. However, the surface modelling functions in most CAD/CAM systems do not minimize the measured errors generated in the digitising process. Evident errors are common when comparing physical objects with surface models.

To solve these problems, researchers have focused their attention on the development of various solutions to improve the digitisation process and the surface modelling result. The first common idea has moved in the direction of an adaptive digitising strategy.

Following this idea the acquisition pitch should be varied in relation with the complexity of the object shape in order to avoid the presence of redundant punctual information located on non-significant zones such as planes or constant curvature surfaces [4], shortening the digitisation time.

All these approaches start from a first digitisation followed by the construction, under different parametric rules [5], of intermediate models. In this way these methodologies allow to decide which are the zones that need to be re-digitised with a more precise strategies.

While all the approaches proposed in literature need the construction of an intermediate model [6], in this work a different methodology, only based on a direct point cloud analysis, is developed.

2. Approach description

The approach developed in this work starts with an initial raw acquisition of the surface points, obtained with the use of a fast scanning device. In this phase points are collected on pitches with regular mesh along both *X*- and *Y*-axes.

After that, with the help of a more accurate measuring system (for example, a CMM), another scanning step is performed in order to individuate the zones with strong changes in curvature. In the first raw acquisition the proposed method permits to localise the boundary of zones characterized by curvature variations. The second acquisition phase is conducted by employing larger pitches in areas with no significant morphological variations of the surface and by decreasing the dimension of pitches in the areas with significant changes in curvature.

While the traditional approaches are usually based on the development of an intermediate mathematical model, and on the use of semi-automatic procedures to discriminate the zone that need to be deeply rescanned, the proposed approach operates directly on the measured point cloud by applying an automatic selective procedure.

2.1. Measured points indexing

The scanned points acquired in the first raw digitisation are reordered according to their associated *X*–*Z* and *Y*–*Z* planes, creating two different orders. This produces that, during the morphological analysis, the object surface is treated according to two orthogonal direction, the first along *X*-axis and the second along *Y*-axis. This kind of pre-processing phase allows a more simple management of points in the subsequent steps. In fact it permits to work in an ordered set of planes instead of a more complex three-dimensional space (Fig. 1).

2.2. Boundary definition

In this second step the algorithm allows to define the boundaries for the more accurate rescanning phase. The procedure is developed along *X*-axis for all the planes individuated in correspondence of each *Y*-value and along *Y*-axis for all the planes individuated in correspondence of each *X*-value [7].

The geometrical parameter used in the algorithm is the angle γ between two subsequent segments obtained by three successive points measured along the same axis, as, for example, given a plane Y_j:$P_{i,j} \equiv (X_{i,j},Z_{i,j})$, $P_{i+1,j} \equiv (X_{i+1,j}, Z_{i+1,j})$ and $P_{i+2,j} \equiv (X_{i+2,j},Z_{i+2,j})$ evaluated on *X*-axis (Fig. 2).

Referring to Fig. 2, if we define as $\alpha_{i,j}$ the inclination angle, with respect to the horizontal axis, of the first segment ($P_{i,I} - P_{i+1,j}$) and as $\alpha_{i+1,j}$ the inclination angle of the subsequent segment, $\gamma_{i,j}$ angle can be obtained by the

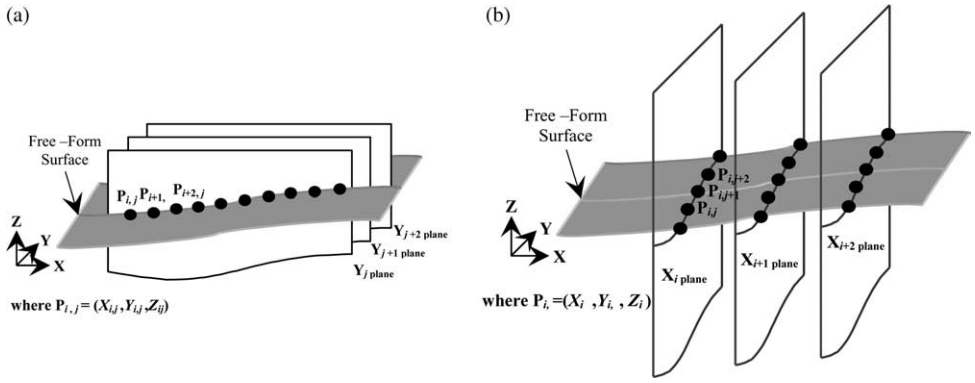

Fig. 1. Measured points indexing: (a) according to *X–Z* planes, (b) according to *Y–Z* planes. Points scanned in the first digitisation phase are reordered according to their associated *X–Z* and *Y–Z* planes. Hence, the surface can be treated according to two orthogonal direction, respectively, along *X* and *Y*-axes.

difference:

$$\gamma_{i,j} = \alpha_{i+1,j} - \alpha_{i,j} \tag{1}$$

$\alpha_{i,j}$ and $\alpha_{i+1,j}$ angles can be evaluated as follows:

$$\alpha_{i,j} = \operatorname{arctg}\left(\frac{Z_{i+1,j} - Z_{i,j}}{X_{i+1,j} - X_{i,j}}\right) \tag{2}$$

$$\alpha_{i+1,j} = \operatorname{arctg}\left(\frac{Z_{i+2,j} - Z_{i+1,j}}{X_{i+2,j} - X_{i+1,j}}\right) \tag{3}$$

Therefore, $\gamma_{i,j}$ angle can be obtained by:

$$\gamma_{i,j} = \operatorname{arctg}\left(\frac{Z_{i+2,j} - Z_{i+1,j}}{X_{i+2,j} - X_{i+1,j}}\right) - \operatorname{arctg}\left(\frac{Z_{i+1,j} - Z_{i,j}}{X_{i+1,j} - X_{i,j}}\right) \tag{4}$$

From a nominal point of view, if $\gamma_{i,j}$ angle is approximately the same for every value of index i it means that the considered points make part of the same line with constant curvature in plane Y_j (Fig. 3). Hence, there is no need of further measures for better evaluating the object curvature in that zone. It must be noted that this is true under the assumption of absence of sudden curvature variation between two subsequent points (that means working with smooth surfaces). This hypothesis is automatically verified when working with free-form surfaces and an adequate acquisition pitch.

Therefore, in order to give the procedure a more strict coherence with the real behaviour of the measurement devices, it is necessary also to consider the presence of the measurement uncertainty.

$\gamma_{i,j}$ angle overall uncertainty can be evaluated starting from single point measurement uncertainties and utilising the following composition law [8]:

$$U(\gamma_{i,j}) = 2u(\gamma_{i,j}) = 2\sqrt{\sum_{l=1}^{N}\sum_{m=1}^{N}\frac{\partial\gamma_{i,j}}{\partial\xi_l}\frac{\partial\gamma_{i,j}}{\partial\xi_m}u(\xi_l,\xi_m)}$$

$$= 2\sqrt{\sum_{l=1}^{N}\left(\frac{\partial\gamma_{i,j}}{\partial\xi_l}\right)^2 u^2(\xi_l) + 2\sum_{l=1}^{N-1}\sum_{m=i+1}^{N}\frac{\partial\gamma_{i,j}}{\partial\xi_l}\frac{\partial\gamma_{i,j}}{\partial\xi_m}u(\xi_l,\xi_m)} \tag{5}$$

where: $\gamma_{i,j}$ is a function of $N=6$ variables ξ_1 ($\xi_1 \equiv X_{i+1,j}$, $\xi_2 \equiv X_{i,j}$, $\xi_3 \equiv X_{i+2,j}$, $\xi_4 \equiv X_{i+1,j}$, $\xi_5 \equiv Z_{i,j}$, $\xi_6 \equiv Z_{i+2,j}$); $U(\gamma_{i,j})$ is $\gamma_{i,j}$ extended uncertainty (expressed at 95% confidence level); $u(\gamma_{i,j})$ is $\gamma_{i,j}$ standard deviation; $u(\xi_l,\xi_m)$ is variable ξ_1 and ξ_m covariance; $u^2(\xi_l)$ is variable ξ_1 variance.

The correlation level between ξ_1 and ξ_m is defined by the correlation coefficient:

$$r(\xi_l, \xi_m) = \frac{u(\xi_l, \xi_m)}{u(\xi_l)u(\xi_m)} \tag{6}$$

where $r(\xi_l,\xi_m) = r(\xi_m,\xi_l)$ and $-1 < r(\xi_l,\xi_m) < 1$.

If ξ_1 and ξ_m are independent, then $r(\xi_l,\xi_m) = 0$, for every $l \neq m$. The covariance terms of Eq. (5) can be written as a function of the correlation coefficient in the following way:

$$2\sum_{l=1}^{N-1}\sum_{m=i+1}^{N}\frac{\partial\gamma_{i,j}}{\partial\xi_l}\frac{\partial\gamma_{i,j}}{\partial\xi_m}u(\xi_l,\xi_m)$$

$$= 2\sum_{l=1}^{N-1}\sum_{m=i+1}^{N}\frac{\partial\gamma_{i,j}}{\partial\xi_l}\frac{\partial\gamma_{i,j}}{\partial\xi_m}u(\xi_l)u(\xi_m)r(\xi_m,\xi_l) \tag{7}$$

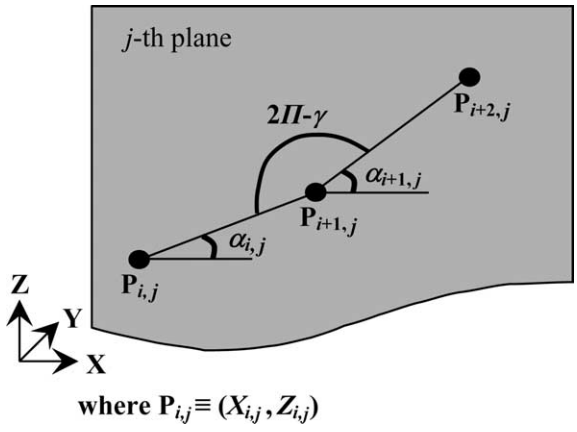

Fig. 2. Geometrical parameter. The geometrical parameter used in the algorithm is the angle γ between two subsequent segments obtained by three successive points measured along the same axis. For example, for given a plane Y_j:$P_{i,j} \equiv (X_{i,j},Z_{i,j})$, $P_{i+1,j} \equiv (X_{i+1,j},Z_{i+1,j})$ and $P_{i+2,i} \equiv (X_{i+2,j}, Z_{i+2,j})$ evaluated on *X*-axis.

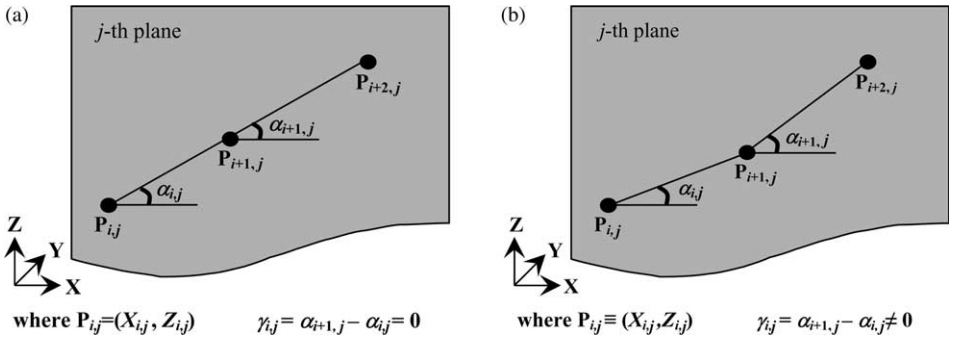

Fig. 3. Example of two different values of $\gamma_{i,j}$ angle: (a) planar zone, (b) non-planar zone. From a nominal point of view if $\gamma_{i,j}$ angle is zero, it means that the three considered points make part of the same straight line in plane Y_j. Otherwise, they come from a curve line. In general, as a first approximation, if two subsequent values $\gamma_{i,j}$ and $\gamma_{i+1,j}$ along the some section of surface are different, that means that there is a change in curvature.

Hence Eq. (5) becomes:

$$U(\gamma_{i,j})=2u(\gamma_{i,j})$$
$$=2\sqrt{\sum_{l=1}^{N}\frac{\partial\gamma_{i,j}}{\partial\xi_l}u^2(\xi_l)+2\sum_{l=1}^{N-1}\sum_{m=i+1}^{N}\frac{\partial\gamma_{i,j}}{\partial\xi_l}\frac{\partial\gamma_{i,j}}{\partial\xi_m}u(\xi_l)u(\xi_m)r(\xi_l,\xi_m)} \quad (8)$$

If all the input variables are correlated with a correlation coefficient $r(\xi_l,\xi_m)=1$, the above equation becomes:

$$u^2(\gamma_{i,j})=\left(\sum_{l=1}^{N}\frac{\partial\gamma_{i,j}}{\partial\xi_l}u(\xi_l)\right)^2 \quad (9)$$

Due to the fact that the points acquired on the surface are correlated, the standard deviation $u(\gamma_{i,j})$ of $\gamma_{i,j}$ angle along all the working planes is:

$$u(\gamma_{i,j})=\left(\frac{\partial\gamma_{i,j}}{\partial Z_{i,j}}\right)u(Z_{i,j})+\left(\frac{\partial\gamma_{i,j}}{\partial Z_{i+1,j}}\right)u(Z_{i+1,j})$$
$$+\left(\frac{\partial\gamma_{i,j}}{\partial Z_{i+2,j}}\right)u(Z_{i+2,j})+\left(\frac{\partial\gamma_{i,j}}{\partial X_{i,j}}\right)u(X_{i,j})$$
$$+\left(\frac{\partial\gamma_{i,j}}{\partial X_{i+1,j}}\right)u(X_{i+1,j})+\left(\frac{\partial\gamma_{i,j}}{\partial X_{i+2,j}}\right)u(X_{i+2,j}) \quad (10)$$

Given that the measurement uncertainty of the scanning device can be considered constant along the three Cartesian axes, it is possible to make some simplification on the mathematical formalisation above. For example, for the $Y_{j\text{th}}$

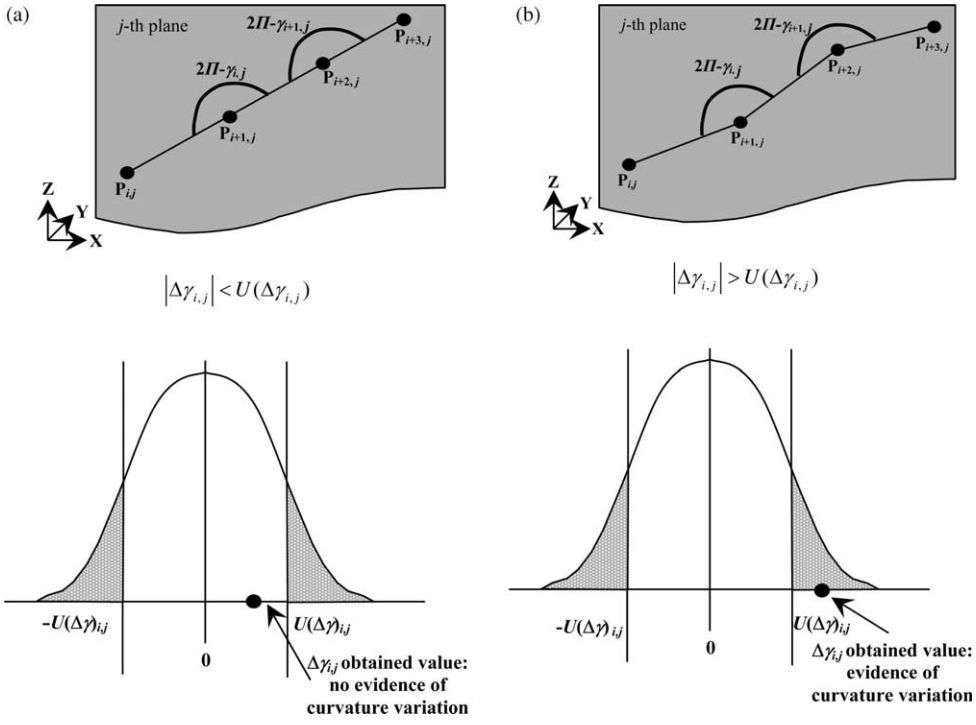

Fig. 4. Example of two cases of curvature variation ($\Delta\gamma_{i,j}$) analysis: (a) no evidence of curvature variation, (b) evidence of curvature variation. There is evidence of curvature variation only if obtained values of $\Delta\gamma_{i,j}$ are external of the interval $\pm U(\gamma_{i,j})$ of the expected distribution.

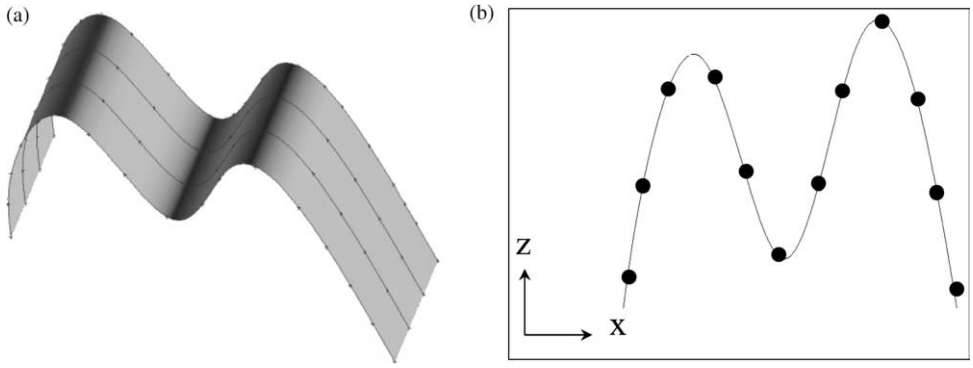

Fig. 5. Surface for the sensitivity test: (a) points cloud obtained in a simulated acquisition on an ideal free-form surface with given curvature variations, (b) one of the four X–Z sections of the surface (Y_1 plane). This surface has been analyzed in order to evaluate the sensitivity of the method in terms of the measurement uncertainty and the surface morphology.

plane:

$$u(Z_{i,j}) = u(Z_{i+1,j}) = u(Z_{i+2,j}) = u(X_{i,j}) = u(X_{i+1,j}) = u(X_{i+2,j}) = u_{\text{const.}} \tag{11}$$

and relation (10) becomes:

$$u(\gamma_{i,j}) = u_{\text{const.}} \left[\left(\frac{\partial \gamma_{i,j}}{\partial Z_{i,j}} \right) + \left(\frac{\partial \gamma_{i,j}}{\partial Z_{i+1,j}} \right) + \left(\frac{\partial \gamma_{i,j}}{\partial Z_{i+2,j}} \right) + \left(\frac{\partial \gamma_{i,j}}{\partial X_{i,j}} \right) + \left(\frac{\partial \gamma_{i,j}}{\partial X_{i+1,j}} \right) + \left(\frac{\partial \gamma_{i,j}}{\partial X_{i+2,j}} \right) \right] \tag{12}$$

The related overall uncertainty (at 95% confidence level) is [8]:

$$U(\gamma_{i,j}) = 2 \cdot u(\gamma_{i,j}) \tag{13}$$

The difference between two subsequent values of angle γ is:

$$\Delta\gamma_{i,j} = \gamma_{i+1,j} - \gamma_{i,j} \tag{14}$$

The corresponding uncertainty can be evaluated by the already mentioned composition law [8], obtaining ($\gamma_{i,j}$ and $\gamma_{i+1,j}$ are strictly correlated):

$$U(\Delta\gamma_{i,j}) = 2[u(\gamma_{i+1,j}) - u(\gamma_{i,j})] \tag{15}$$

As a consequence of this, we can individuate a variation of curvature only if obtained values of $\Delta\gamma_{i,j}$ are external of the interval $\pm U(\Delta\gamma_{i,j})$ (Fig. 4).

3. Experimental validation

In a first phase, the method has been tested using an ideal geometry. The acquisition process has been simulated by generating a set of measurement points on a known surfaces (specifically a free-form surface characterized by a significant curvature variation). This has been done in order to evaluate the sensitivity of the method in terms of the measurement uncertainty and the surface morphology.

The surface has been generated employing the B-spline curve formalisation [9] (see Fig. 5).

$$p(u) = \sum_{i=0}^{n} p_i N_{i,k}(u) \quad \text{with } n = 5 \text{ and } k = 3 \tag{16}$$

After analyzing the results collected on different surfaces generated by the same formula (16), but with different curvature values (angle γ), ranging from 0.008 till 3 rad, the test has confirmed that the sensibility of the method is directly correlated to the measurement uncertainty of the scanning device $u_{\text{cost.}}$: small values of uncertainty produce elevate sensibility. Considering, for example, the value $u_{\text{cost.}} = 0.025$ mm, the method is able to discriminate a curvature variation ($\Delta\gamma$) larger than 0.2 rad. This means that surfaces with curvature variation smaller or equal to 0.2 rad will be considered, as a first approximation, with constant

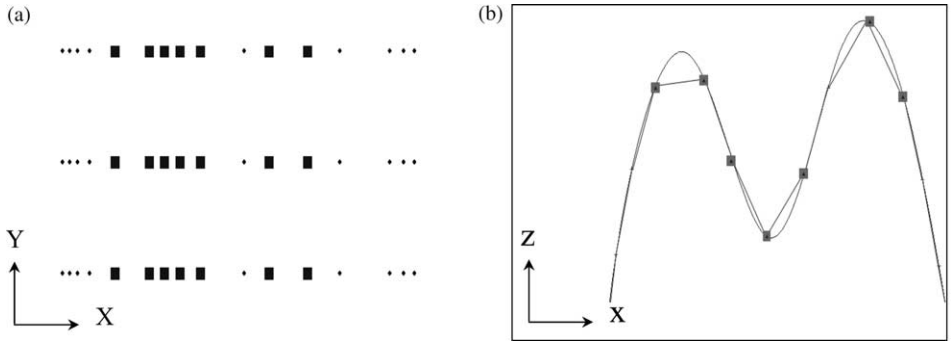

Fig. 6. Area definition on X–Y plane: (a) X–Y plane projection, (b) one of the four X–Z sections of the surface (Y_1 plane). The boundaries in the X–Y plane (evidenced squares) localise the most significant curvature variations in the X-direction.

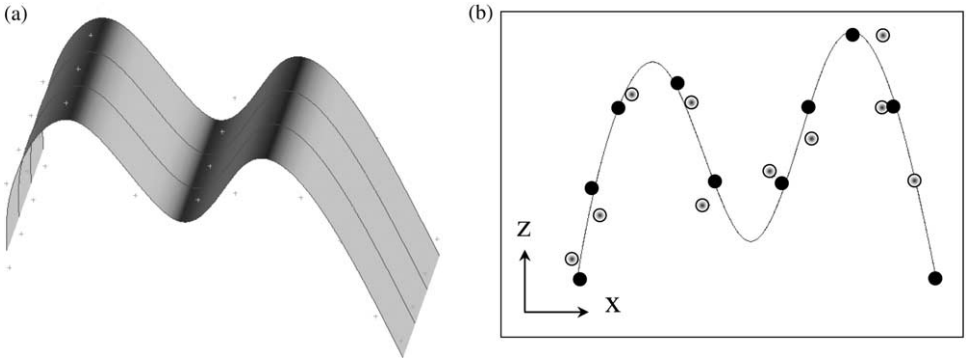

Fig. 7. Testing free-form surface with noise: (a) points cloud on the surface, (b) one of the four X–Z sections of the surface (Y_1 plane). Points (grey circles) has been obtained with a simulated acquisition on an ideal free-form surface introducing a Gaussian perturbation simulating the measurement uncertainty.

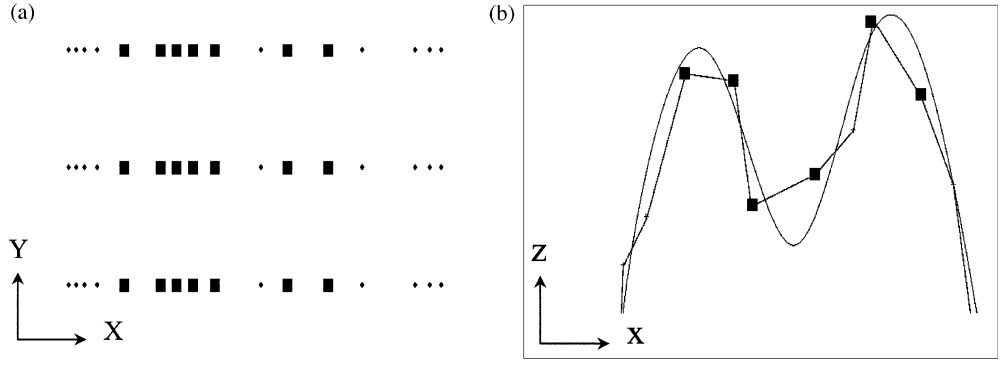

Fig. 8. Area definition on X–Y plane (after introducing a Gaussian perturbation in acquired data): (a) X–Y plane projection, (b) one of the four X–Z sections of the surface (Y_1 plane). The boundaries in the X–Y plane (evidenced squares) localise the most significant curvature variations in the X direction.

curvature. Fig. 6 shows the results obtained by analyzing curvature variation of surface in Fig. 5 along its X–Z sections.

A successive test lies in introducing a Gaussian perturbation into the coordinate values of the acquired surface points, in order to simulate the variability due to the measurement uncertainty (see Fig. 7).

The perturbation amplitude has been imposed of the same entity of the uncertainty of a real measurement device ($u_{\text{cost.}} = 0.025$ mm). The application results of the method are reported in Fig. 8.

In a second phase of this study, the surface of a sample object with a specific shape has been digitised with the use of the laser scanning system Minolta VIVID 900, in order to develop an experimental validation of the procedure. Data acquisition system is based on two main components: a digital camera (CCD) and a source that project a laser blade on the object (see Fig. 9).

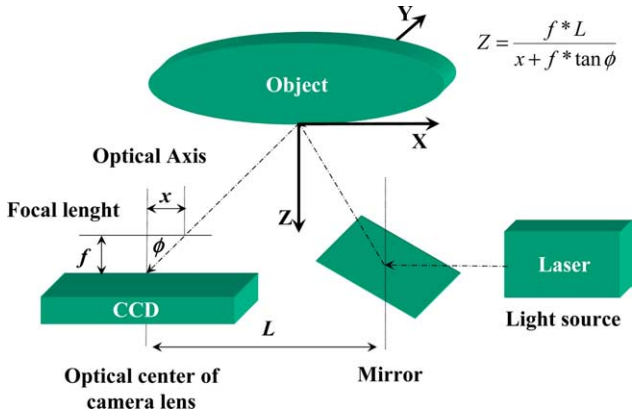

Fig. 9. Laser Scanner digitisation methodology. Scheme of the acquisition system used for the digitisation of the analysed sample surface.

Fig. 10. Object sample (human face) used for the validation test. A human face has been used for the methodology validation.

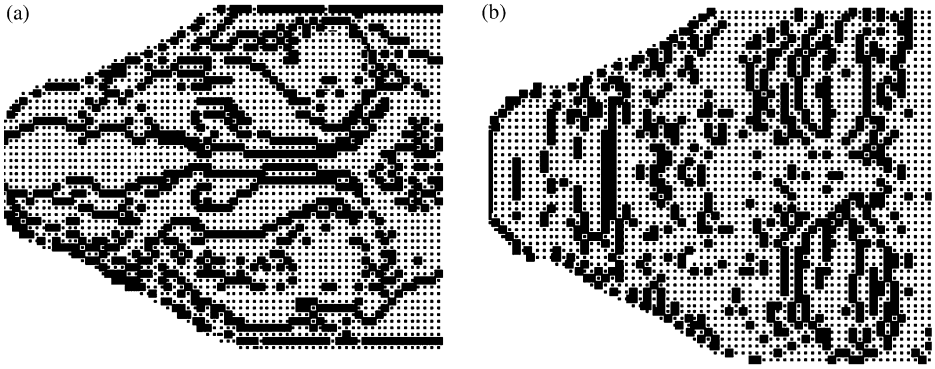

Fig. 11. Area definition in *X*–*Y* plane: (a) due to curvature variation in *Y* planes, (b) due to curvature variation in *X* planes. The zones (evidenced stars) localise the most significant curvature variations, respectively, in the *X*- and *Y*-directions.

The position along *Z*-axis of the scanned points is given by:

$$Z_P = \frac{f \times L}{x + f \times \tan \phi} \tag{17}$$

where (see Fig. 9): x represents the reflected point position on the sensor; ϕ is the reflecting angle of the laser bundle; L is separating line between the lens and deflected source; f is the effective distance between the sensor position and the lens.

The orientations of X and Y coordinates automatically come from the scanning matrix pitch.

An effective sample for the validation of the proposed methodology is a human face [10,11]. Looking at the morphology of this surface (Fig. 10) it is easy to see that the most significant zones, in term of curvature variation, are the eyes, the mouth and the nose of the represented face. The other regions of the object does not show any significant morphological variations and can be considered like constant-curvature zones.

As a consequence, the algorithm should evidence those zones as the regions which need a deeper curvature analysis.

A first digitisation of the surface has been performed using a 0.4×0.4 mm^2 pitch. Considering the specific laser scanner device uncertainty, as declared by the constructor, $U_S = 2 \cdot u_{cost} = 0.05$ mm, the overall uncertainty for every $\gamma_{i,j}$ angle can be calculated using Eqs. (12) and (13). At this point the curvature analysis has been performed point by point using the obtained value of $U(\Delta\gamma_{i,j})$ as discriminating threshold.

Looking at the results (Fig. 11), a good level of coherence is shown between the expected regions and the individuated zones with significant curvature variations.

In order to look at the sensibility of the model, a further experimental step has been run: the discriminating threshold has been forced to different values by imposing different levels of the instrument uncertainty. A first result obtained with an uncertainty value of 0.04 mm (lower than the real one) gives rise to some unexpected zones which do not correspond to the real morphology of the sample surface (Fig. 12). This behaviour is justified by the fact that the uncertainty of the instrument is higher than the used parameter and for that reason a great amount of measurement noise is caught.

A second result, obtained with an uncertainty value of 0.06 mm (higher than the real one), gives rise to significant resolution problems (Fig. 13). This could be showed by the absence of evidence over some zones in which a real curvature variation should be expected.

4. Conclusions

The paper describes an automatic procedure for selective identification of sampling points in reverse engineering applications. The aim is to individuate the boundaries of curvature variation zones, which need a further scansion by a more accurate device and with a smaller dimension of pitches. The methodology is based on the curvature analysis of sample surface.

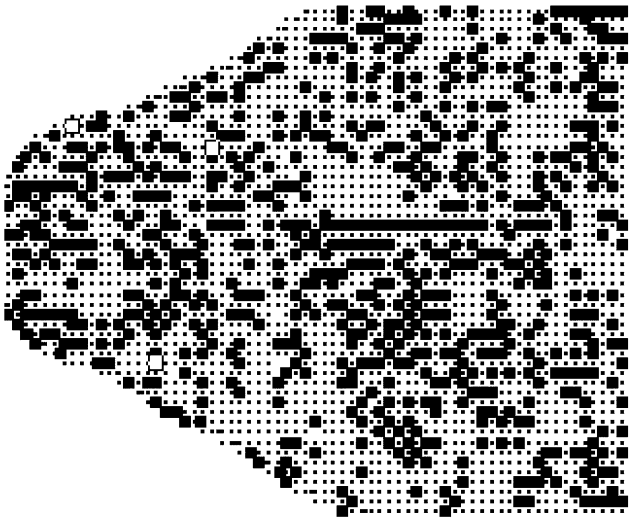

Fig. 12. Wrong area definition. Imposing an instrument uncertainty value of 0.04 mm (lower than the real one) gives rise to some unexpected zones which do not correspond to the real morphology of the sample surface.

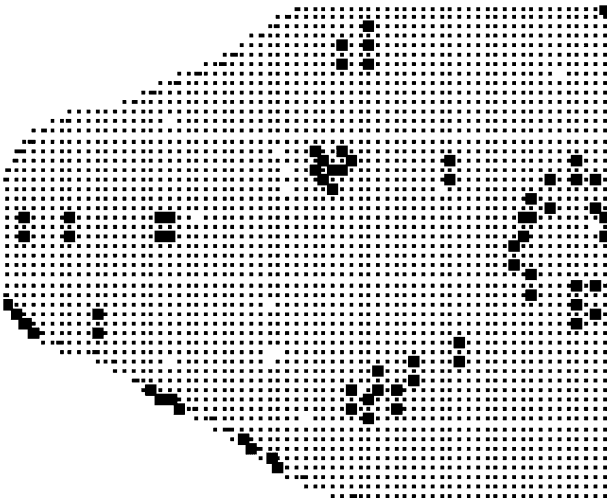

Fig. 13. Wrong area definition. Imposing an instrument uncertainty value of 0.06 mm (higher than the real one) gives rise to significant resolution problems. This is showed by the absence of evidence over some zones in which a real curvature variation should be expected.

The discrimination between zones with different curvature is carried out by using the metrological characteristics of the inspection device. In particular, a threshold value for the difference of inclination angles between two subsequent sampling intervals is defined on the basis of the inspection device measurement uncertainty.

The methodology has been applied to different kind of free-form patterns. Looking at the obtained results, it is possible to say that this procedure has a good level of applicability in automated scansion systems. The use of scanning device measurement uncertainty turns out a general purpose procedure for identification of critical zones without operator involvement.

The sensibility of the method depend on the first scanning pitch dimension, on the measurement system measurement uncertainty and on the smoothness of the tested surface.

Experiments conducted with discrimination thresholds lower than that based on the measurement uncertainty show the appearance of unexpected curvature zones, which do not correspond to the real morphology of the sample surface. On the other hand, higher threshold values produce the loss of some significant curvature zones.

The methodology described in this paper has been applied to a plane-by-plane bi-dimensional analysis of the scanned surface. This is an elementary algorithm for curvature definition, but, in general, the method could be extended to any other kind of more complicated approach. The future work will be dedicated to a direct three-dimensional approach, which consists of meshing the entire point cloud and analysing the relative inclination between the planes identified by adjacent triangles. In fact, the use of two sets of coordinate planes (X–Z and Y–Z), which as a first approximation works effectively, could be, however, misleading, the result might depend on the current position and orientation of the object in the measuring arrangement.

References

[1] B. Bidanda, K. Harding, Reverse engineering: an evaluation of prospective non contact technologies and applications in manufacturing systems, International Journal of Computer Integrated Manufacturing 30 (10) (1991) 791–805.

[2] Y. Chen, X. Tang, Automatic digitisation of free-form curve by coordinate measuring machines, ASME: PED, Engineered Surfaces 62 (1992) 139–148.

[3] F. Xi, Error compensation for the 3D line laser scanning data, International Journal of Advanced Manufacturing and Technology 32 (1994) 120–128.

[4] L. Chen, An integrated reverse engineering approach to reconstructing free—from surfaces, Computer Integrated manufacturing Systems 10 (1) (1997) 49–60.

[5] L. Iuliano, E. Vezzetti, Comparison of Reverse Engineering Techniques for Jewellery Prototyping, AITEM (Associazione Italiana Tecnologia Meccanica), Brescia, 1999. pp. 231–240.

[6] S. Motavalli, A part image reconstruction system for reverse engineering of design modifications, Journal of Manufacturing Systems 10 (5) (1991) 383–395.

[7] G. Farin, Curvature and fairness of curves and surfacess, IEEE Computer Graphics and Applications 9 (1989) 52–57.

[8] BIPM, IEC, ISCC, ISO, IUPAC, IUPAP, OIML, Guide to the Expression of Uncertainty in Meas-urement, ISO publication, Genève, 1993.

[9] M. Morteson, Modelli Geometrici in Computer Graphics, McGraw-Hill, Milan, 1989.

[10] J.P. Moss, A laser scanner system for the measurements of facial surface morphology, Journal of Optic and Lasers in Engineering 10 (1989) 179–190.

[11] J.P. Moss, (1988) Non contact measurement using a laser scanning probe, SPIE In process Optical Measurements, No. 1012, 229–239.